Nanoscale

Accepted Manuscript

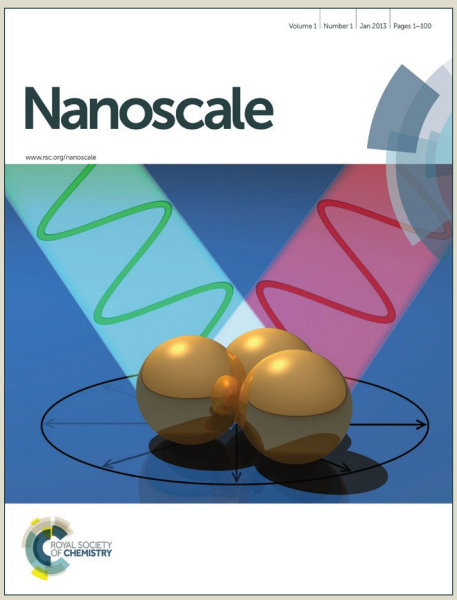

ROYAL SOCIETY OF CHEMISTRY

www.rsc.org/nanoscale

Journal Name

ARTICLE

Zinc oxide nanorod assisted rapid single-step process for conversion of electrospun poly(acrylonitrile) nanofibers to carbon nanofibers with high graphitic content

Received 00th January 20xx,
Accepted 00th January 20xx

DOI: 10.1039/x0xx00000x

www.rsc.org/

Ratyakshi Nain, Dhirendra Singh, Manjeet Jassal and Ashwini K. Agrawal

The effect of incorporation of rigid zinc oxide (ZnO) nanostructures on carbonization behavior of electrospun special acrylic fiber grade poly(acrylonitrile) (PAN-SAF) nanofibers was investigated. ZnO nanorods with high aspect ratio were incorporated in PAN-*N,N*-dimethylforamide system and the composite nanofibers reinforced with aligned ZnO rods upto 50 wt% were successfully electrospun, and subsequently, carbonized. The morphology and the structural analysis of the resultant carbon nanofibers revealed that the rigid ZnO nanorods, present inside the nanofibers, possibly acted as scaffolds (temporary support structures) for immobilization of polymer chains and assisted in uniform heat distribution. This facilitated rapid and efficient conversion of the polymer structure to the ladder, and subsequently, the graphitized structure. At the end of the process, the ZnO nanorods were found to completely separate from the carbonized fibers yielding pure carbon nanofibers with high graphitic content and surface area. The approach could be used to eliminate the slow, energy intensive stabilization step and achieve fast conversion of randomly laid carbon nanofiber webs in a single step to carbon nanofibers without the application of external tension or internal templates usually employed to achieve high graphitic content in such systems.

Introduction

Carbon nanofibers (CNFs) because of their high mechanical strength, stiffness, modulii, high corrosion resistance, excellent thermal and electrical conductivity offer applications in various areas including nanoelectronics,[1] nanophotonics,[2] filtration,[3,4] fuel cells/rechargeable batteries,[5,6] supercapacitors,[7-9] high performance composites[10] and as templates for synthesis of hierarchical nanostructures.[11]CNF can be produced by conventional chemical vapour deposition,[12,13] hot filament assisted sputtering,[14] high density plasma induced chemical vapour deposition,[15] template assisted synthesis,[16,17] and carbonization of various precursors including poly(acrylonitrile) (PAN),[18,19] pitch,[20] rayon,[21] polyvinylpyrrolidone,[22] etc.

Electrospinning is one of the most effective techniques used for producing carbon nanofibers from PAN. However, CNF produced from electrospinning lack optimized molecular orientation in the fibers. Application of tension during thermal treatment particularly during stabilization is crucial for production of mechanically strong CNF. Most of the reports[9.23] available have used random electrospun fiber-webs as precursor of CNF. Due to their random nature, it is usually difficult to apply necessary tension or stretch during the conversion process.

Various approaches that have been used for application of tension or stretching, as reported in the literature, are wrapping a bundle of aligned electrospun nanofibers on a glass rod[24] and hot stretching a sheet of nanofibers clamped between two graphitic plates.[25]

Another approach of improving microstructure of CNF is to help graphitization during the carbonization process. For this, graphitic nanostructures such as carbon nanotube (CNT)[26-28] and graphene oxide particles[29] have been incorporated in PAN precursor nanofibers, which were shown to have a global templating effect during carbonization, wherein the formation of graphitic structure was found to propagate from the CNT templates to the surrounding CNF material. This effect was prominent at high carbonization temperature of 1200 to 1800 °C.

All of the above mentioned approaches require a slow two-step process of heat treatment. First step is a stabilization process carried out at 200-300 °C in air, which converts/oxidizes PAN polymer structure to the ladder structure and the second step is carbonization process carried out at high temperature of 800 to 1500 °C, which converts the ladder structure to the carbon structure. The ratio of random to ordered structure in the carbon fibers is the most important criterion for judging the quality of the carbon fibers and is

[a] *SMITA Research Lab, Department of Textile Technology, Indian Institute of Technology Delhi, Hauz Khas, New Delhi -110016, India*

† Electronic Supplementary Information (ESI) available: The Scanning electron micrographs (SEM) of electrospun composite PAN nanofibers, separated ZnO nanorod white mass, TGA curves for PAN and ZnO-PAN composite nanofibers and Raman spectra of precursor and carbonized composite nanofibers. XRD spectrum of ZnO nanorods See DOI: 10.1039/x0xx00000x

usually a function of heating rate, stabilization temperature, and tension applied during the stabilization.

We have recently reported a method of incorporating anisotropic zinc oxide (ZnO) nanostructures inside PAN nanofibers.[30] Interaction of ZnO nanostructures with polymer chains and solvent was observed to play a crucial role in achieving their dispersion within the fiber and alignment along the nanofiber axis. The method allowed inclusion of highly aligned substantial quantities of ZnO rods in the range of 10 wt% to 50 wt% on the weight of PAN in the nanofibers. The polymer chains in the dried fibers were found to have strong interaction with the dispersed and aligned ZnO rods. Unlike CNT, which have very small diameter, and therefore, have a tendency to easily bend and entangle with each other to form clusters that are difficult to disperse and align, ZnO nanorods are stiff and can be easily dispersed and aligned in nanofibers. It is hypothesized that the presence of large amounts of dispersed and aligned ZnO nanorods in the nanofibers may control the movement of polymeric chains surrounding these nanorods, and hence, could significantly influence their stabilization and subsequent carbonization behavior.

In the present study, effect of the presence of ZnO nanorods on structure development during carbonization process of PAN-SAF nanofibers (obtained using special acrylic fiber grade polymer) has been investigated.

Experimental

Materials

Special acrylic terpolymer (PAN-SAF referred to as PAN in the manuscript), with average M_w of 1,29,000, was procured from Technorbital Advanced Materials Pvt. Ltd. (Kanpur, UP, India). The terpolymer had methyl acrylate and methacrylic acid as comonomers in addition to acrylonitrile. Zinc acetate dihydrate, sodium hydroxide (NaOH), *N,N*-dimethylforamide (DMF), and ethanol were procured from Merck, India.

Synthesis of ZnO rods

The nano sized ZnO rods were synthesized using hydrothermal non stirred vessel as reported in the literature.[31-33] Zn^{2+} / OH^- ratio was kept at 1:10 and ethanol was used as solvent for the synthesis. In a typical procedure, zinc acetate dihydrate ($Zn(Ac)_2.2H_2O$) (0.002 moles) was added in 20 ml ethanol. In the above dispersion, 0.02 moles of NaOH dissolved in 40 ml ethanol were added drop wise. This mixture was then transferred to a non-stirred hydrothermal vessel and kept for 12 h at 150 °C. Precipitates obtained were washed several times with water, finally with ethanol and then dried.

Dispersion of ZnO rods in DMF

As reported in our previous study,[30] DMF was found to be a good solvent for dispersing ZnO rods in PAN solution. The ZnO rods (10, 20, 30 and 50 wt% on the weight of PAN) were dispersed in DMF by stirring for 15 min followed by ultrasonication for 30 min (Elma, at 100% power and frequency of 35 kHz). Concentrated PAN solution in DMF (10 wt%) was added in the above dispersion of ZnO rods to adjust the total solid contents to 5 wt%. The solution was homogenized by stirring it for 3 h followed by sonication for 30 min at the frequency of 35 kHz.

Electrospinning

Electrospinning was carried out using an infusion syringe pump KDS 100 (KD Scientific, Holliston, United States) and a flat tip needle (internal diameter 0.834 mm). High voltage dual polarity power supply (40 kV), Model-DES40PN from Gamma HV (Florida, United States), was used to charge the needle as well as a collector plate. The polymer solutions with and without homogeneously dispersed ZnO rods were electrospun at a fixed flow rate of 0.5 ml/h. The distance from the tip of needle to the collector was kept at 15 cm. The temperature and relative humidity was maintained at 30 °C, 40%, respectively. This arrangement resulted in randomly laid nanofiber webs, which were dried in vacuum oven and used for characterization. The fibers obtained with 10, 20, 30, 50 wt% of ZnO rods were coded as 10 ZnO-PAN, 20 ZnO-PAN, 30 ZnO-PAN and 50 ZnO-PAN, respectively.

Stabilization and carbonization of nanofibers

The electrospun nanofibers were converted to carbon fibers in 2 steps using a conventional process.

The first step was oxidative stabilization, which involved heating the fibers to 280 °C at a ramp rate of 2 °C/min in air and holding them at this temperature for 1 h. In the second step, these fibers were taken to 400, 700 and 1000 °C in nitrogen atmosphere at a ramp rate of 5 °C/min to attain carbonization. The effect of temperature on carbonization was investigated on PAN and 30 ZnO-PAN fibers. PAN fiber samples, where both stabilization and carbonization steps were involved as mentioned above, were coded as PANOX-400, PANOX-700, PANOX-1000, respectively. Similarly, 30 ZnO-PAN composite fibers, which were subjected to both stabilization and carbonization treatment as above, were coded as 30 ZnO-PANOX-400, 30 ZnO-PANOX-700 and 30 ZnO-PANOX-1000. Similarly, the samples with different ZnO nanorod content of 10, 20, 30, 50 wt% on weight of PAN were electrospun, followed by the oxidation and carbonization, as described above and were coded as 10 ZnO-PANOX-1000, 20 ZnO-PANOX-1000, 30 ZnO-PANOX-1000 and 50 ZnO-PANOX-1000 for carbonization till 1000 °C.

In the modified single step approach of carbonization, the separate step of oxidative stabilization was eliminated and the precursor PAN and ZnO-PAN nanofibers were directly heated from room temperature to 1000 °C at a heating rate of 5 °C/min in N_2 atmosphere. These samples were coded as PAN-1000, 10 ZnO-PAN-1000, 20 ZnO-PAN-1000, 30 ZnO-PAN-1000 and 50 ZnO-PAN-1000 for PAN nanofibers containing 0, 10, 20, 30 and 50 wt% of ZnO rods, respectively.

Characterization

The morphology of ZnO rods and electrospun fibers was determined using a field emission scanning electron microscope (FE-SEM), FEI Quanta 200F, Eindhoven, The Netherland. The diameter of the nanofibers was determined as an average of 200 readings using Image J software. X-ray diffraction (XRD) patterns for ZnO nanorods were obtained using X-ray diffractometer, X'Pert Pro,

PANalytical (Almelo, Netherlands). Scanning transmission electron microscopy and Energy dispersive X-ray (EDX) mapping for various elements was carried out using X-max 80 mm^2, Oxford Instruments (Oxfordshire, UK) to determine presence and distribution of ZnO nanorods inside the precursor and carbonized nanofibers. The thermal stability of nanofibers was characterized using Thermo gravimetric analyzer (TGA), (Model TGA Q500). Thermal transitions were characterized using Differential scanning calorimetry (DSC), (Model-DSC Q200, TA Instruments, New Castle, DE, USA). Samples of 5-10 mg electrospun fibers were quenched at -20 °C, followed by heating up to 300 °C at a heating rate 3 °C/min under nitrogen atmosphere at a flow rate 50 ml/min. The modulation was done with step size of 1 °C/min every 60 s. The fibers were also characterized using confocal laser dispersion micro Raman spectrometer (Model-INVIA, laser 514 nm^{-1}, Renishaw, Gloucestershire, UK). The peaks corresponding E_{2g2} mode at 1580 cm^{-1} (G peak) for ordered graphitic crystallites of carbon and bands associated with amorphous sp^2-bonded carbons and interstitial defects at 1360 cm^{-1} (D peak) and 1534 cm^{-1} (D" peak) were deconvoluted using Wire 3.2 software to determine I_D/I_G ratio using the following formula:

I_D/I_G = (Integrated intensities of D + D" peaks)/Integrated intensity of G peak

The mechanical properties of PAN and ZnO reinforced PAN nanofiber webs were measured using Instron microtensile tester (Model-5848, Singapore). For tensile properties the electrospun fibers were deposited on a 5 × 5 cm template for 5 min and softly rolled into a bundle like structure. The samples were fixed on a window template axially with the help of a scotch tape. 10 N load cell was used with gauge length of 25 mm and cross-head speed of 50 mm/min. An average of 10 measurements is reported.

Results and Discussion

Morphology of ZnO-PAN composite fibers

The morphology of ZnO rods and PAN nanofiber webs was analyzed using STEM and FE-SEM as shown in Figures 1 and S1 (Supporting Information). The synthesized ZnO rods had an average diameter of 50 ± 10 nm with a length of 0.7 ± 0.2 microns. XRD analysis showed presence of highly pure wurtzite hexagonal phase in ZnO nanorods (Figure S2 in supporting information). PAN nanofibers had an average diameter of 250 ± 50 nm. The fiber diameter of PAN-ZnO composites was found to increase to 600 ± 50 nm, 700 ± 100 nm, 900 ± 100 nm as the amount of ZnO rods was increased to 10 wt% (10 ZnO-PAN), 20 wt% (20 ZnO-PAN) and 30 wt% (30 ZnO-PAN). However, further increase in ZnO rods to 50 wt% (50 ZnO-PAN) resulted in decrease of the diameter to 600 ± 100 nm.

It may be noted that the total solid content (PAN + ZnO rods) in all solutions taken for electrospinning was kept constant at 5 wt%. This means that samples containing increasing amounts of ZnO have correspondingly lower concentrations of polymer in the solution. These are mentioned in Table 1. STEM images (Figure 1) and FE-SEM images (S1) of the composite fibers show that the ZnO nanorods are dispersed inside the PAN nanofibers. None of the ZnO nanostructure could be observed outside the nanofibers.

Table 1 Composition of spinning solutions used for making precursor nanofibers.

Sample	ZnO (wt.%) on wt. of polymer	Polymer (wt.%) in spinning solution	Diameter of nanofibers (nm)
PAN	0	5.00	250 ± 50
10 ZnO-PAN	10	4.55	600 ± 50
20 ZnO-PAN	20	4.17	700 ± 100
30 ZnO-PAN	30	3.85	900 ± 100
50 ZnO-PAN	50	3.33	600 ± 100

Further, the EDX mapping of Zn, O and C elements was carried out to trace the location of ZnO rods and is shown in Figure 2. EDX mapping showed homogenous distribution of carbon over the entire image of the nanofibers. On the other hand, zinc (Zn) and oxygen (O) elements were found to be present only at the locations were ZnO rods were seen in the SEM images. The observations confirmed that the ZnO nanorods were not only dispersed inside the nanofibers but were also aligned along their axes resulting in reinforced nanostructures. These results are similar to those reported in our earlier study on textile grade PAN nanofibers.[30] In nanofibers reinforced with 10 wt% and 20 wt% ZnO rods, the rods were properly dispersed inside the fibers without any overlapping. In nanofibers with 30 wt% ZnO rods, again the rods were uniformly dispersed inside fibers with a little overlapping of rods inside the fibers. However, nanofibers with 50 wt% ZnO rods showed prominent overlapping of ZnO rods due to very high loading (Figure 1). Though the polymer content in the spinning solutions was lower with higher ZnO content, the significant increase in diameter of the nanofibers with incorporation of ZnO rods was attributed to the change in elasticity and viscosity of the spinning solutions due to strong interaction between PAN chains and the rods. At smaller addition of ZnO at 10-30 wt%, the individual rods were able to interact well with the polymer and probably were able to create an elastic networked structure. However, at higher loadings of 50 wt%, stacking/aggregation of rods could interfere in creating this elastic structure resulting in somewhat lower diameter of 600 ± 100 nm, similar to that of 10 ZnO-PAN nanofibers.

Interestingly, this value is still much larger than that of the pure PAN nanofibers even though the spinning solution has much lower concentration of polymer at 3.33 wt%. As described in our previous report, ZnO rods have tendency to align along the nanofiber axis because of their interaction with both the solvent as well as polymer chains.[30]

Effect of ZnO nanorods on mechanical properties of composite nanofibers

The mechanical properties of PAN and ZnO reinforced PAN electrospun nanofibers is shown in Figure 3. The ZnO incorporation was found to increase the mechanical strength as well as the modulus of the composite electrospun fibers. Compared to PAN nanofiber web, 10 ZnO-PAN nanofiber web showed marginal improvement from 6.5 ± 1.2 MPa to 6.9 ± 0.6 MPa and 74 ± 15 MPa to 83 ± 6 MPa in breaking stress and modulus, respectively. ZnO

content of 20 wt% in 20 ZnO-PAN resulted in significant improvement to 9.5 ± 3.3 MPa and 203 ± 83 MPa, respectively. 30 ZnO-PAN nanofiber web were found to exhibit the tensile strength of 11 ± 1.9 MPa and modulus of 321 ± 72 MPa. Increase of the ZnO content to 50 wt% (50 ZnO-PAN) did not result in further improvement of mechanical properties and the tensile strength and modulus of the nanoweb remained nearly same at 11.6 ± 4.8 MPa and 325 ± 40 MPa, respectively.

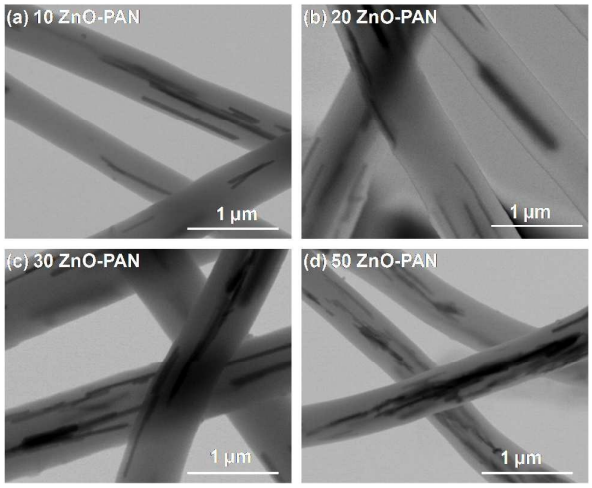

Figure 1 STEM images of electrospun nanofibers (a) 10 ZnO-PAN (b) 20 ZnO-PAN (c) 30 ZnO-PAN and (d) 50 ZnO-PAN.

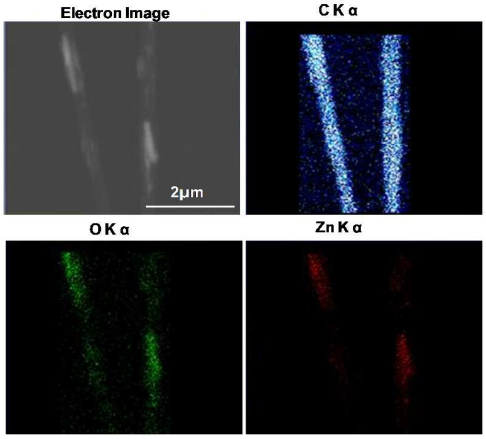

Figure 2 EDX mapping of 30 ZnO-PAN precursor nanofibers.

However, the extension was observed to decrease with increase in amount of ZnO nanorods. This indicated that presence of ZnO nanorods imposed significant restriction on the movement of polymer chains in the composite fibers.

Effect of ZnO on thermal behavior of composite fibers

Figure 4 shows the DSC curves for PAN and ZnO-PAN nanofiber samples for reversible and irreversible heat flow. PAN nanofibers were observed to exhibit a clear first glass transition (T_g) at 85.5 °C and melting temperature (T_m) of PAN at 268 °C. The incorporation of 10 wt% of ZnO rods resulted in increase in T_g to 87.5 °C.

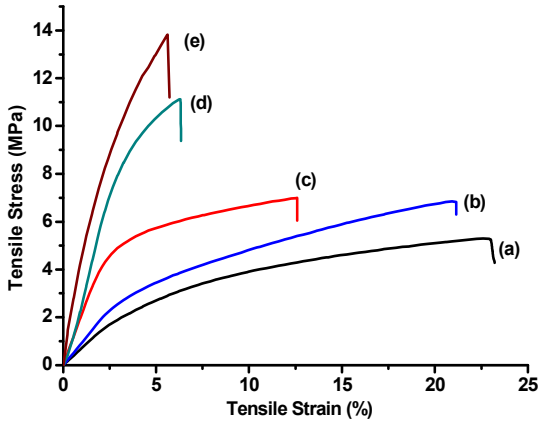

Figure 3 Tensile stress-strain curves for (a) PAN (b) 10 ZnO-PAN (c) 20 ZnO-PAN (d) 30 ZnO-PAN and (e) 50 ZnO-PAN.

Incorporation of higher amounts of ZnO nanorods (30 and 50 wt%) resulted in a very broad T_g extending to ~116 °C. The increase in T_g indicated that the molecular mobility of polymer chains in composite fibers were highly restricted in the presence of ZnO nanorods.

The melting peaks seen in reversible heat flow curves are small with an enthalpy of 7-10 J/g (Table 2). This is due to the fact that polymer chains of PAN undergo simultaneous exothermic reactions such as cyclization, dehydrogenation and oxidation in the same temperature range to form cyclized ladder type structure. The exothermic peak seen in the irreversible heat flow curves correspond to the above reactions. In PAN nanofibers, the cyclization peak appeared at 271 °C and enthalpy of cyclization was 477 J/g. Addition of ZnO rods resulted in only a marginal shift of the peak towards higher temperature of 273 °C. However, the intensity of exothermic peak increased substantially with large increased in the enthaphy of cyclization to 524 J/g, 613 J/g and 713 J/g with increase in ZnO content to 10, 30 and 50 wt%. The higher enthalpy values of cyclization indicate that the stabilization reaction of PAN could proceed to a greater extent in the presence of ZnO rods. The higher intensity and lower FWHM of these peaks further indicate that the reactions have proceeded at a higher rate. These observations may be attributed to the restricted molecular mobility of the PAN chains in the presence of ZnO rods. It is hypothesized that in the presence of rigid ZnO rods, the polymer chains may remain oriented and in extended conformation to allow higher extent of cyclization in a shorter time. This observation is in conformity with reported studies in the literature,[34-35] where the stretching/tension on PAN precursor fibers during stabilization could result in improved release of exothermic heat. The incorporation of ZnO nanorods also improved the thermal stability of the ZnO-PAN nanofibers (Figure S3 in supporting information). The effect of ZnO rods in ZnO-PAN composite precursor nanofibers is in contrast to the effect of additives and monomers used in conventional precursors, where these are incorporated to initiate the cyclization reaction at a lower temperature and to broaden the exothermic peak.

Table 2 Thermal properties of ZnO-PAN nanofiber.

Sample	Melting (reversible)		Cyclization (irreversible)		
	T_m (°C)	ΔH_m (J/g)	T_{cyc} (°C)	ΔH_{cyc} (J/g)	FWHM (°C)
PAN	268	7.5	271	477	16.4
10 ZnO-PAN	269	8.5	273	524	15.8
30 ZnO-PAN	271	9.9	273	613	14.3
50 ZnO-PAN	270	10.2	273	713	14.7

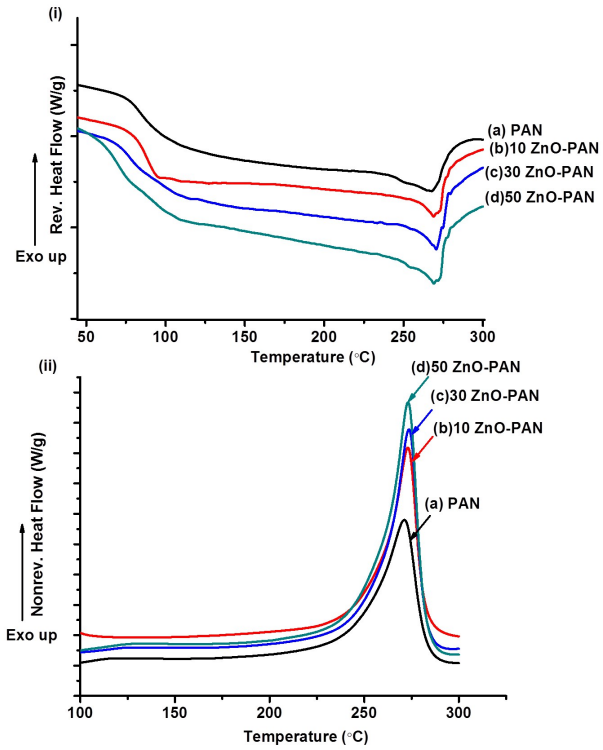

Figure 4 DSC curves for PAN and ZnO-PAN composite nanofibers (i) reversible heat flow (ii) irreversible heat flow.

Effect of ZnO on carbonization behavior of composite precursors

30 ZnO-PAN nanofibers with well dispersed ZnO rods having some overlapping of rods were selected to investigate the effect of carbonization temperature on the structure formation. Sample of PAN nanofibers was taken as a control. These samples were processed in conventional two steps. First, all the samples were stabilized under same conditions i.e. by heating them at low heating rate of 2 °C/min in air and holding them at 280 °C for 1 h.

These were, subsequently, carbonized under nitrogen environment by heating them to different temperatures of 400, 700 and 1000 °C.

The SEM micrographs of the resultant nanofibers are shown in Figure 5. The fibers (PANOX-400) obtained from PAN (control) were found to have diameter of 227 ± 25 nm after carbonization at 400 °C. The diameter further decreased to 204 ± 24 nm and 156 ± 17 nm on increasing the carbonization temperature to 700 °C (PANOX-700) and 1000 °C (PANOX-1000), respectively. The surface of the fibers was smooth. 30 ZnO-PAN fibers carbonized at 400 °C (30 ZnO-PANOX-400) and 700 °C (30 ZnO-PANOX-700) were found to have ZnO nanorods present inside the fibers. The diameters of these fibers were 839 ± 72 nm and 690 ± 144 nm, respectively. However, when the sample was heated to 1000 °C (30 ZnO-PANOX-1000), the ZnO nanorods could not remain inside the fiber and were found to be expelled yielding pure carbon fiber of diameter 237 ± 150 nm. On carbonization to 1000 °C, the treated sample was found to have web of carbon nanofibers and separated white particles/mass.

FE-SEM analysis did not show any entrapment of ZnO nanorods inside the carbon nanowebs, whereas the separated white particles were found to be aggregated mass of ZnO nanorods. The SEM image of the white mass is shown in supporting information (Figure S4). The physical separation of nanorods into a white mass may have been facilitated due to unidirectional flow of nitrogen during the carbonization process. The STEM images of the carbonized fibers also did not show any trace of ZnO nanorods inside the nanofibers (example is shown in Figure 6). When the surface of the fibers were observed at a higher magnification under FE-SEM, they were observed to have several elongated nanocavities (Figure 7) of the size similar to that of ZnO nanorods and oriented along the fiber axis. These appeared to have formed due to the expulsion of embedded nanostructures. EDX mapping of the samples was carried out to determine the purity of the CNFs obtained from composite ZnO-PAN nanofibers.

The EDX mapping (Figure 8) showed the presence of carbon (C) element at all the locations where CNFs were seen in the SEM images. However, there was no trace of zinc (Zn), which confirmed the complete expulsion of ZnO nanorods to yield pure CNFs. Traces of oxygen element, which can be seen over the entire scanned area, irrespective of the location of the CNFs, may have arisen due to the background/absorbed oxygen.

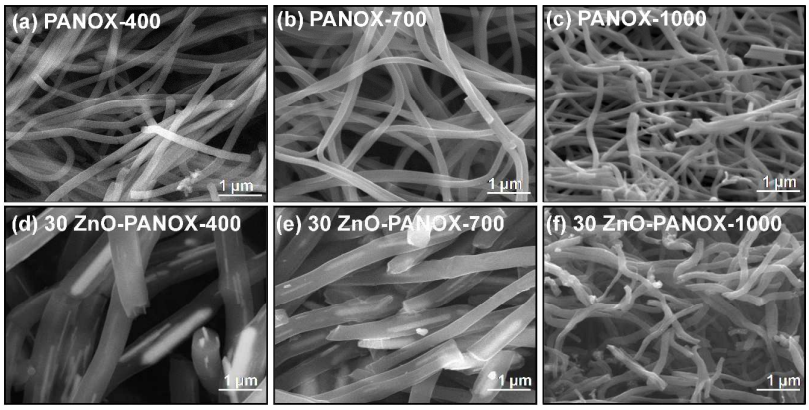

Figure 5 FE-SEM micrographs of (a) PANOX-400 (b) PANOX-700 (c) PANOX-1000 (d) 30 ZnO-PANOX-400 (e) 30 ZnO-PANOX-700 and (f) 30 ZnO-PANOX-1000.

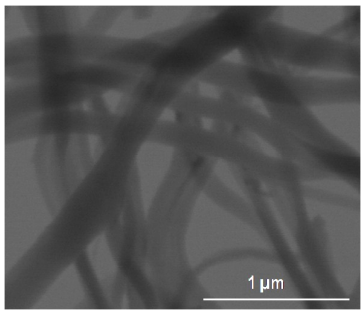

Figure 6 STEM micrographs of 30 ZnO-PANOX-1000 carbonized fibers.

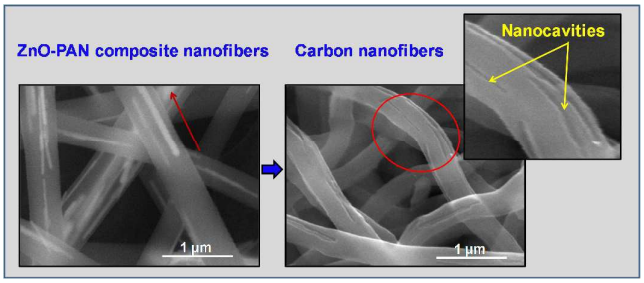

Figure 7 Scanning electron micrographs of ZnO-PAN composite fibers and the generated carbon fibers with nanocavities.

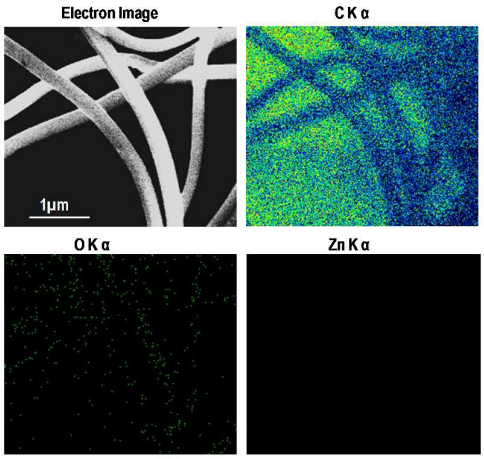

Figure 8 EDX mapping of carbon nanofibers obtained from 30 ZnO-PAN composite nanofibers.

Effect of ZnO rods on the carbonization behavior of PAN electrospun fibers was studied using Raman spectroscopy. The spectra given in Figure 9, were deconvoluted using typical Gaussian–Lorentzian peaks for carbon fibers. These corresponded to Raman allowed E_{2g2} mode at 1580 cm^{-1} (G peak) for ordered graphitic crystallites of carbon and bands associated with amorphous sp^2-bonded carbons and interstitial defects at 1360 cm^{-1} (D peak) and 1534 cm^{-1} (D" peak).

It was observed that in case of both control PANOX and 30 ZnO-PANOX nanofibers, the intensity of peak corresponding to graphitic content (~1580 cm^{-1}) i.e. the ordered sp^2 bonded carbon atoms increased with the increase in carbonization temperature.

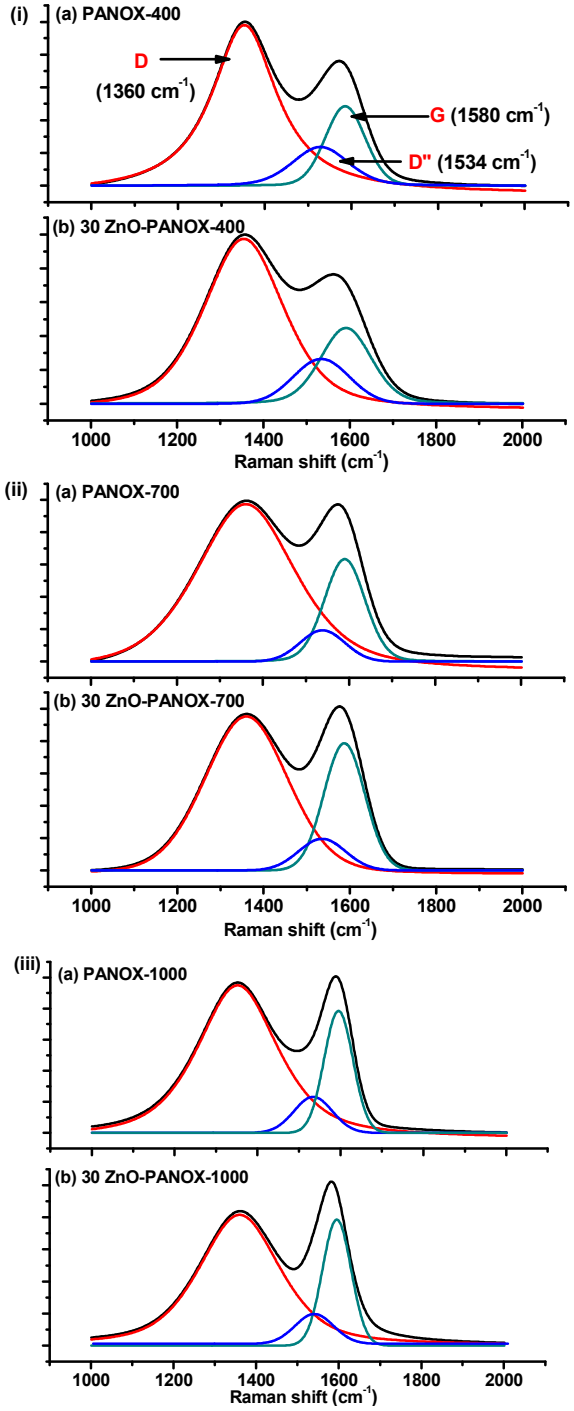

Figure 9 Raman spectra of (a) PANOX and (b) 30 ZnO-PANOX heat treated to (i) 400 °C (ii) 700 °C (iii) 1000 °C.

This observation is in conformity with the reported literature for PAN carbon nanofibers.[24] Integrated intensity (i.e. area) of D band (I_D) is proportional to the number of scattering disordered carbon atoms and integrated intensity (i.e. area) of G band (I_G) is proportional to that of ordered sp^2 bonded carbon atoms in the illuminated region. Figure 10 shows I_D/I_G ratios of carbon nanofibers obtained at different carbonization temperatures.

I_D/I_G value was found to decrease with increase in carbonization temperature in both PANOX and 30 ZnO-PANOX carbon fibers indicating increase in their graphitic content. The higher graphitic content observed at higher temperature is a result of both the temperature used and the time taken to reach the carbonization temperature.

In PANOX carbon fibers, I_D/I_G ratio decreased marginally from 4.97 at 400 °C to 4.62 at 1000 °C, whereas in 30 ZnO-PANOX, the values changed significantly from 4.04 to 2.42, respectively (Table 3). Interestingly, even at the carbonization temperature of 400 °C, 30 ZnO-PANOX 400 has much lower I_D/I_G value compared to PANOX 1000. This indicates an active role of ZnO nanorods on carbonization behavior of the composite fibers.

Effect of ZnO content on carbonization behavior

Among the various carbonization temperatures studied for 30 ZnO-PANOX, carbonization at 1000 °C yielded pure carbon fibers without the presence of ZnO rods. This infers that the role of ZnO nanorods can only be realized below 1000 °C.

Therefore, this temperature was selected to investigate the influence of the amount of ZnO nanorods in precursor PAN nanofibers on their carbonization behavior. PAN precursor nanofibers containing 0, 10, 20, 30, and 50 wt% on the weight of PAN were used for carbonization study. The samples were processed in two steps as described earlier-first stabilized in air at 280 °C for 1 h to obtain oxidized PAN (PANOX) nanofibers and were then taken to 1000 °C in nitrogen to obtain carbonized nanofibers. The morphology of the obtained carbon nanofibers was analyzed using FE-SEM as shown in Figure 11. Carbon nanofibers obtained from PAN precursor had uniform surface.

However, all of the carbon nanofibers produced from ZnO-PAN composite precursors were found to have several elongated nanocavities along the fiber axis as described in the earlier section. Since these cavities appeared to have formed due to the expulsion of ZnO nanorods, their number increases with increased percentage of ZnO content in the precursor.

The effect of ZnO wt% on diameter of carbonized PAN nanofibers in comparison to their precursor's diameters is shown in Figure 12. The diameter of the carbon nanofibers increases from 156 ± 17 nm obtained from PAN precursor to 309 ± 43 nm in 10 ZnO-PANOX-1000 and further to 339 ± 40 nm in 20 ZnO-PANOX-1000. However, on increasing the ZnO content to 30 wt% and 50 wt%, the diameters decreased to 237 ± 150 nm and 220 ± 48 nm, respectively.

Table 3 Raman peak analysis for samples carbonized at different temperatures.

Sample	Peak Position (FWHM) in cm^{-1}		I_D/I_G
	I_D	I_G	
PANOX-400	1353 (182)	1586 (109)	4.97
PANOX-700	1359 (274)	1589 (111)	4.77
PANOX-1000	1352 (230)	1595 (81)	4.62
30 ZnO-PANOX-400	1354 (220)	1591 (138)	4.04
30 ZnO-PANOX-700	1360 (229)	1587 (111)	2.79
30 ZnO-PANOX-1000	1360 (231)	1586 (90)	2.42

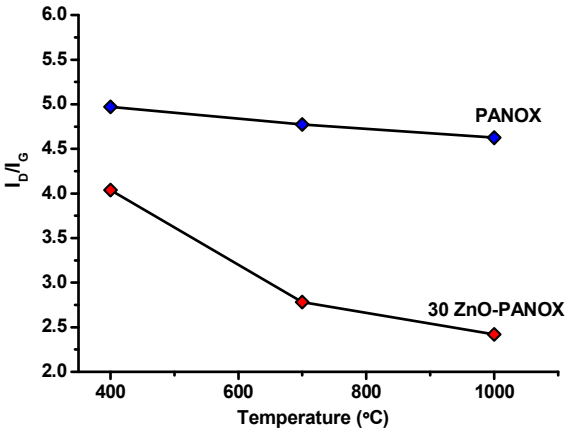

Figure 10 Effect of carbonization temperature on I_D/I_G ratio of PANOX and 30 ZnO-PANOX fibers.

The decrease in diameters of the carbon nanofibers with respect to their precursor diameters can be ascribed to the mass loss due to carbonization process and the removal of ZnO nanorods from the carbonized fibers.

Figure S5 (Supporting Information) shows Raman spectra (1000–2000 cm^{-1}) of carbonized fibers along-with deconvoluted peaks for G (1580 cm^{-1}), D (1360 cm^{-1}) and D" (1534 cm^{-1}) bands. The integrated intensity (area) of G band peak, which is characteristic of ordered graphitic phase, was found to increase in comparison to the disordered carbon band D with the increase in ZnO content in precursor fibers from 10 to 50 wt%.

Based on the correlation given by Tuinstra–Koenig,[36] Knight and White[37] have developed empirical formula for calculating crystallite domain size of graphite (L_a) from the R value (i.e. I_D/I_G), which is given below:

$$\boldsymbol{R = \frac{I_D}{I_G} = \frac{C(\lambda)}{L_a}} \qquad (1)$$

Where, C is a function of laser wavelength λ and is usually taken as 4.4 nm for 514 nm^{-1} laser.

$$\boldsymbol{L_a(nm) = \frac{4.4}{R}}$$

According to Umair et al.,[38] this commonly used prefactor of 4.4 is not valid in general, and hence, should be derived for the laser using the following equation:

$$\boldsymbol{C = 560/E_{laser}{}^4 = 2.4 \times 10^{-10}\lambda_{Laser}} \qquad (2)$$

Using the above equation, the prefactor for 514 nm^{-1} laser is calculated to be 16.75.

Both the values of L_a determined using the two prefactors suggested by Knight and Umair are listed in Table 4. PANOX-1000 carbon nanofibers obtained with oxidative stabilization step showed a high I_D/I_G ratio of 4.62. This high value was expected because the fibers were heat-treated in the form of random nanofiber webs without the application of external tension. This would allow the polymer chain to relax with application of heat and result in a randomized carbon structure.

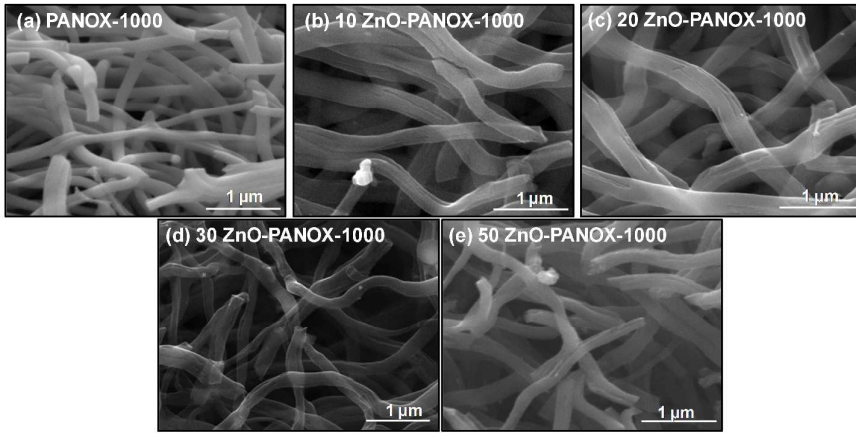

Figure 11 SEM images of carbon nanofibers (a) PAN-1000 (b) 10 ZnO-PANOX-1000 (c) 20 ZnO-PANOX-1000 (d) 30 ZnO-PANOX-1000 and (e) 50 ZnO-PANOX-1000.

Compared to the I_D/I_G ratio of PANOX-1000, the I_D/I_G ratio of 10 ZnO-PANOX-1000 was found to be significantly lower at 2.99. The further increase in ZnO content in the precursor fibers resulted in gradual decrease in this ratio to 2.31 in 50 ZnO-PANOX-1000. The increase in ZnO content in precursors also resulted in substantial increase in crystallite domain size (L_a) of graphite phase by more than 100% from 0.952 nm in PANOX-1000 to 1.905 nm in 50 ZnO-PANOX-1000.

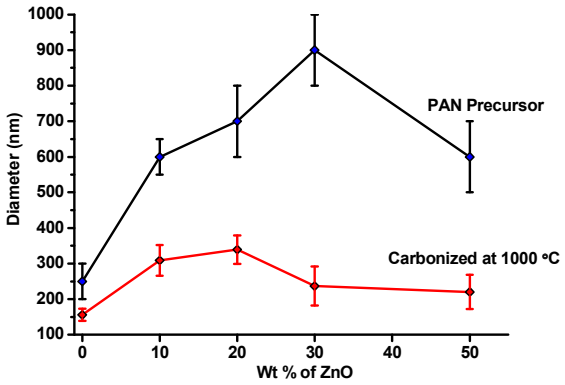

Figure 12 Diameters of precursor and carbonized PANOX nanofibers.

The corresponding L_a values using Umair method ranged from 3.57 nm to 7.19 nm. The decrease in the I_D/I_G values and the corresponding increase of L_a values on incorporation of ZnO rods suggested substantial increase in size and content of graphitic structures in the resultant carbon nanofibers. This nature of improvement in the graphitic content of carbon fibers is usually attributed to the applied tension during their stabilization process. The tension tends to keep the polymer chains extended to facilitate the formation of ladder structure, which eventually yields ordered graphitic structure on carbonization. The similar increase in the graphitic content observed in the random nanowebs of the present study, processed without any form of externally applied tension, suggests that the presence of ZnO nanorods inside the polymer matrix might be playing a crucial role during stabilization.

Table 4 Comparison of properties of carbon nanofibers obtained by single and two-step process.

Sample	Peak Position (FWHM) in cm^{-1} I_D	I_G	I_D/I_G	L_a (nm) Knight	L_a (nm) Umair
Two-step process					
PANOX-1000	1352 (230)	1595 (81.6)	4.62	0.952	3.57
10 ZnO-PANOX-1000	1358 (246)	1589 (87)	2.99	1.472	4.93
20 ZnO-PANOX-1000	1359 (252.5)	1587 (90.9)	2.70	1.63	5.84
30 ZnO-PANOX-1000	1360 (231)	1586 (90)	2.42	1.818	6.81
50 ZnO-PANOX-1000	1361 (229)	1592 (90)	2.31	1.905	7.19
Single-step process					
PAN-1000	1350 (230.8)	1598 (87.1)	4.69	0.938	3.63
10 ZnO- PAN-1000	1361 (258.5)	1587 (89.7)	3.40	1.294	5.60
20 ZnO- PAN-1000	1359 (255)	1587 (89)	2.87	1.533	6.20
30 ZnO- PAN-1000	1361 (231)	1589 (89)	2.46	1.789	6.92
50 ZnO- PAN-1000	1361 (226)	1592 (90)	2.33	1.888	7.25

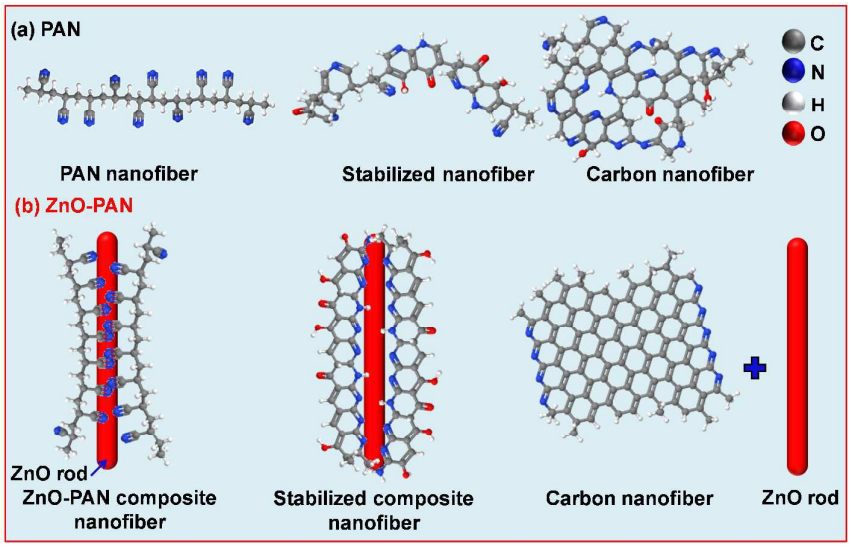

Figure 13 Carbonization mechanisms for PAN and ZnO-PAN composite nanofibers.

The rigid nanostructures are likely to immobilize the polymer chains surrounding them and assist in keeping them oriented during the stabilization process. This immobilization may be due to the strong interaction between the ZnO rods and the polymers chains.[30] This is clearly indicated in the Raman spectra of PAN and 30-ZnO-PAN precursor nanofibers (Figure S6, Supporting Information), which show a significant shift of wavenumber for -CN stretching peak from 2246 to 2252 cm^{-1}.

The interaction of -CN groups with ZnO might also facilitate alignment of nitrile groups towards the ZnO nanorod surface, thereby, bringing them in favorable conformation for efficient cyclization reaction seen in this study. During the condensation process, the nitrile groups from different chains facing the ZnO nanorods combine to form cyclized structure. This forces the rigid ZnO nanostructures to move away to facilitate the cyclization process. As more and more number of the polymer chains come close and condense into a bigger graphitic structure, the ZnO nanorods are slowly pushed out of the carbon matrix. Also, as the carbonization process proceeds, the elimination of nitrogen from the ladder structure would reduce the interaction of the cyclized chains with the ZnO nanorods, which may further facilitate their separation from the carbonized matrix. This proposed mechanism has been shown schematically in Figure 13. With the increase in the content of these rigid nanostructures, the fraction of polymer chains experiencing the above effect is likely to increase, and hence, would result in overall better graphitic structure.

Another interesting observation is that though the diameters of the precursor fibers increased considerably (by 140-260%) with incorporation of ZnO nanorods, they still resulted in formation of better graphitic structure. This is in contrast to the conventional process, where the increase in diameter of the precursor fibers often results in deterioration of the ordered carbon regions. This is usually because of the nonuniform distribution of the evolved heat during the stabilization process, which may tend to degrade the structure before carbonization can take place. It appears that the presence of ZnO nanorods may be helping in redistributing the evolved heat to minimize the thermal degradation. Further the presence of ZnO nanorods is likely to help in the formation of fibrillar structure as shown in Figure 14. According to the SEM images, the morphology of the cross-section of the PANOX-1000 nano carbon fibers appears to be solid cylinder without any distinctive feature, while that of 30 ZnO-PANOX-1000 show fibrillar morphology.

Single step rapid process for carbon nanofibers

In order to investigate the extent of role of ZnO in stabilization, the separate stabilization step of heating the sample slowly in air and holding it at 280 °C for 1 h, as described in the above section, was eliminated. Instead, the precursor nanofibers were subjected to a single step heat treatment at a faster rate of 5 °C/min from the room temperature to 1000 °C in nitrogen atmosphere to obtain carbon nanofibers.

The morphology of the obtained carbon nanofibers was analyzed using FE-SEM as shown in Figure 15. Similar to the two step process, the carbon nanofibers obtained from PAN precursor had uniform surface, whereas, those from ZnO-PAN composite precursors had several elongated nanocavities along the fiber axis. Their number of cavities increased with increased percentage of ZnO content in the precursor.

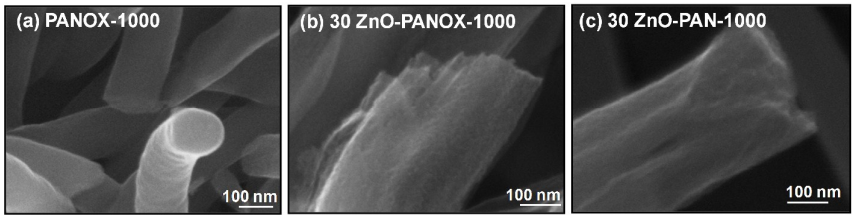

Figure 14 FE-SEM images of carbon nanofibers (a) PANOX-1000 (b) 30 ZnO-PANOX-1000 and (c) 30 ZnO-PAN-1000.

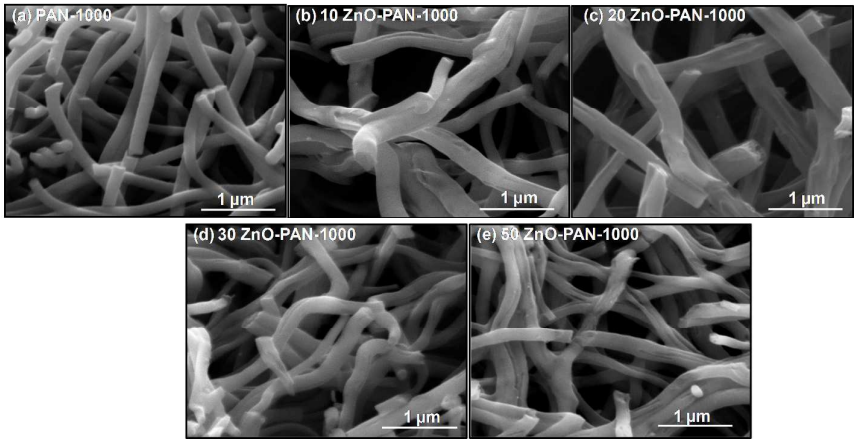

Figure 15 SEM images of carbon nanofibers (a) PAN-1000 (b) 10 ZnO-PAN-1000 (c) 20 ZnO-PAN-1000 (d) 30 ZnO-PAN-1000 and (e) 50 ZnO-PAN-1000.

The diameters of the carbon nanofibers obtained with the single-step process were in the same range as that of the two-step conventional process. The diameter of the carbon fiber from PAN precursor was 194 ± 24 nm, from 10 ZnO-PAN was 310 ± 51 nm, from 20 ZnO-PAN was 375 ± 76 nm, from 30 ZnO-PAN was 248 ± 94 nm and from 50 ZnO-PAN was 228 ± 44 nm.

Also, the morphology of the carbon nanofibers, as shown in Figure 14, remains fibrillar, which is similar to that of 30 ZnO-PANOX-1000 carbon nanofibers.

Raman analysis was carried out for these fibers using the bands described before. The peak positions of D band, G band, their FWHM values, I_D/I_G ratios and La values are given in Table 4.

Carbonization of PAN precursor without the oxidation step, PAN-1000 also showed high I_D/I_G ratio of 4.69, similar to that of PANOX-1000 (I_D/I_G = 4.62). Since both samples were processed without the application of external tension, these values remained high indicating the formation of disordered carbon structures. A little lower value of I_D/I_G ratio of PANOX-1000 nanofibers, suggests that the important role of stabilization process, which allows the formation of a ladder structure at a lower temperature.

Similar to the observations reported for the two-step process, the incorporation of ZnO has resulted in significantly lower I_D/I_G ratios for all the samples. Also, the values of I_D/I_G ratio were found to decrease with increase in the content of ZnO in the precursor fibers. The I_D/I_G ratio decreased from 3.40 in 10 ZnO-PAN-1000 to 2.33 in 50 ZnO-PAN-1000. As mentioned above, the rigid nanostructures present in the fibers are playing a crucial role by immobilizing the polymeric chains and keeping them oriented during the initial heating process with proper distribution of heat along the fiber. With the increase in the content of these rigid nanostructures, the fraction of polymer chains experiencing the above effect increases, and hence, results in overall better graphitic structure. From the above observations, the role of ZnO in formation of graphitic structure is evident for the samples carbonized in single step. The comparison of the carbonized samples obtained with or without stabilization step is shown in Figure 16.

Figure 16 shows a clear difference in the I_D/I_G ratios for samples obtained with 10 and 20 wt% ZnO nanorods. In these samples, the two-step processing involving the oxidation step resulted in a better graphitization of the precursors. However, on increasing the ZnO content to 30 and 50 wt%, the I_D/I_G ratios were much lower than the above samples and were almost same for the two different processes.

For 30 ZnO-PAN-1000, the I_D/I_G ratio was 2.46 versus 2.42 for 30 ZnO-PANOX-1000. This difference reduced further to give I_D/I_G ratios of 2.33 and 2.31 for 50 ZnO-PAN-1000 and 50 ZnO-PANOX-1000, respectively. The results indicate that the presence of 30 wt% of ZnO nanorods in precursors were sufficient to compensate for the effect of a separate stabilization step.

Needless to say that the graphitic domain sizes also followed the same trend and the samples processed in single step with 30 and 50 wt% ZnO nanorods could result in high domain sizes (L_a = 1.79 nm, 1.89 nm, respectively) similar to the samples processed using two steps (L_a= 1.82, 1.91 nm, respectively).

The peak positions and FWHM values for D and G band do not change significantly suggesting the carbonized samples obtained by the two different processes are similar.

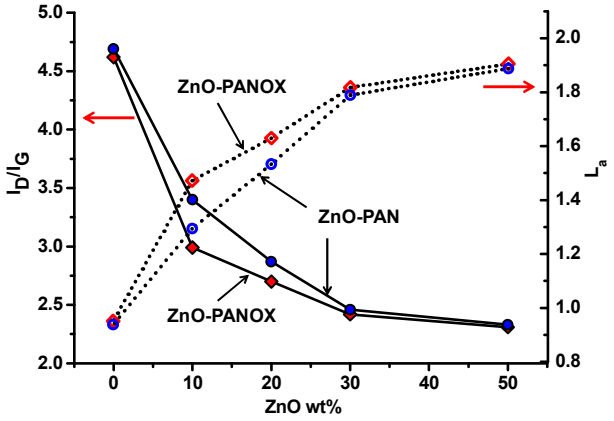

Figure 16 Effect of ZnO content on I_D/I_G ratio and graphitic domain (L_a) of ZnO-PAN-1000 and ZnO-PANOX-1000 carbon fibers.

The above results clearly indicate that the time consuming oxidative stabilization step can be effectively eliminated by incorporating rigid anisotropic nanostructures of ZnO without affecting the graphitic domain size, surface defects or the level of graphitization in the resultant carbon nanofibers.

The results are significant with respect to both the technical quality of the nanocarbon fibers obtained and the economy of the process. It is known that due to the small fiber diameter and the delicate nature of the electrospun PAN nanofibers, it is extremely challenging to improve their graphitic structure on carbonization using conventional approaches. The present process facilitates the formation of pure carbon nanofibers having high graphitic content. The process also provides a simple method for creating higher surface area which is a requirement for certain applications.

The ZnO nanorods used in the process provide scaffolding effect (i.e. temporary structures) to arrest the molecular mobility of the polymer chains during their transformation to graphitic structure, and subsequently, come out of the fibers to yield pure carbon nanofibers. These recovered ZnO nanostructures can be recycled or used for other applications.[39-41] Further, the process allows elimination of stabilization step and significantly faster heating rate, which are extremely important for achieving higher production rate at lower energy cost. The single-step process as used in the above experiments could save ~45% of the process time and ~90% of the energy consumed during the stabilization step.

Conclusions

Composite PAN nanofibers with well dispersed aligned ZnO nanorods were successfully electrospun. The incorporation of ZnO nanorods was found to significantly improve the mechanical properties of the nanowebs. The tensile strength and modulus of the nanowebs with 50 wt% ZnO nanorods increased to 200% and 450%, respectively, compared to the nanowebs without ZnO. The composite nanofibers showed significantly lower extensibility and higher glass transition temperature indicating that the movement of polymer chains was highly restricted by the incorporation of ZnO rods. On carbonization, all the samples with ZnO nanorods were found to have significantly lower I_D/I_G ratios. The I_D/I_G ratio was found to decrease with increasing content of ZnO in the precursor fibers. The values decreased from 4.69 in control sample to 3.40 in samples with 10 wt% ZnO and to 2.33 in samples with 50 wt% ZnO. The rigid ZnO nanostructures present in the fibers played a crucial role by immobilizing the polymeric chains and keeping them oriented during the initial heating process with proper distribution of heat along the fiber. The presence of 30 wt% ZnO nanorods in PAN nanofibers allowed elimination of stabilization step and helped in significantly faster carbonization with better graphitic content. The ZnO nanostructures provided a scaffolding effect during the initial phase of carbonization and were observed to get separated ~ 1000 °C to yield pure carbon nanofibers.

Acknowledgements

Authors would like to acknowledge the partial financial support by the Department of Science and Technology, Govt. of India under various research grants. Authors would also like to thank Technorbital Advanced Materials Pvt. Ltd. for providing us with a free sample of PAN-SAF used in the study.

Notes and references

1. V. I. Merkulov, A. V. Melechko, M. A. Guillorn, D. H. Lowndes and M. L. Simpson, *Applied Physics Letters*, 2001, **79**, 2970-2972.
2. H. Li, L. Pan, Y. Zhang, L. Zou, C. Sun, Y. Zhan and Z. Sun, *Chemical Physics Letters*, 2010, **485**, 161-166.
3. I. Chun, D. H. Reneker, H. Fong, X. Fang, J. Deitzel, N. B. Tan and K. Kearns, *Journal of Advanced Materials*, 1999, **31**, 36-41.
4. C. Park, E. S. Engel, A. Crowe, T. R. Gilbert and N. M. Rodriguez, *Langmuir*, 2000, **16**, 8050-8056.
5. L. Chen, S. Hong, X. Zhou, Z. Zhou and H. Hou, *Catalysis Communications*, 2008, **9**, 2221-2225.
6. J. W. Long, B. Dunn, D. R. Rolison and H. S. White, *Chemical Reviews*, 2004, **104**, 4463-4492.
7. C. Kim, Y.-O. Choi, W.-J. Lee and K.-S. Yang, *Electrochimica Acta*, 2004, **50**, 883-887.
8. S. Mitra, A. K. Shukla and S. Sampath, *Journal of Power Sources*, 2001, **101**, 213-218.
9. C. Kim, B. T. N. Ngoc, K. S. Yang, M. Kojima, Y. A. Kim, Y. J. Kim, M. Endo and S. C. Yang, *Advanced Materials*, 2007, **19**, 2341-2346.
10. L. Wang, Y. Yu, P. C. Chen, D. W. Zhang and C. H. Chen, *Journal of Power Sources*, 2008, **183**, 717-723.
11. H. Hou and D. H. Reneker, *Advanced Materials*, 2004, **16**, 69-73.
12. G. Zou, D. Zhang, C. Dong, H. Li, K. Xiong, L. Fei and Y. Qian, *Carbon*, 2006, **44**, 828-832.
13. J. P. Tu, L. P. Zhu, K. Hou and S. Y. Guo, *Carbon*, 2003, **41**, 1257-1263.
14. K. Kamimura, Y. Mizuno, R. Hayashibe and Y. Onuma, *Molecular Crystals and Liquid Crystals Science and Technology Section A: Molecular Crystals and Liquid Crystals*, 2002, **387**, 163-166.
15. H. W. Wei, K. C. Leou, M. T. Wei, Y. Y. Lin and C. H. Tsai, *Journal of Applied Physics*, 2005, **98,** 1-8.
16. G. Zheng, Y. Yang, J. J. Cha, S. S. Hong and Y. Cui, *Nano Letters*, 2011, **11**, 4462-4467.
17. A. Huczko, *Appl Phys A*, 2000, **70**, 365-376.
18. S. Y. Gu, Q. L. Wu and J. Ren, *Xinxing Tan Cailiao/ New Carbon Materials*, 2008, **23**, 171-175.
19. K. Naito, Y. Tanaka, J.-M. Yang and Y. Kagawa, *Carbon*, 2008, **46**, 189-195.
20. H. Ono and A. Oya, *Carbon*, 2006, **44**, 682-686.
21. H. Rong, Z. Ryu, J. Zheng and Y. Zhang, *Carbon*, 2002, **40**, 2291-2300.
22. P. Wang, D. Zhang, F. Ma, Y. Ou, Q. N. Chen, S. Xie and J. Li, *Nanoscale*, 2012, **4**, 7199-7204.
23. E. Zussman, X. Chen, W. Ding, L. Calabri, D. A. Dikin, J. P. Quintana and R. S. Ruoff, *Carbon*, 2005, **43**, 2175-2185.
24. Z. Zhou, C. Lai, L. Zhang, Y. Qian, H. Hou, D. H. Reneker and H. Fong, *Polymer*, 2009, **50**, 2999-3006.
25. X. Hou, X. Yang, L. Zhang, E. Waclawik and S. Wu, *Materials and Design*, 2010, **31**, 1726-1730.
26. D. Papkov, A. M. Beese, A. Goponenko, Y. Zou, M. Naraghi, H. D. Espinosa, B. Saha, G. C. Schatz, A. Moravsky, R. Loutfy, S. T. Nguyen and Y. Dzenis, *ACS Nano*, 2013, **7**, 126-142.
27. H. Hou, J. J. Ge, J. Zeng, Q. Li, D. H. Reneker, A. Greiner and S. Z. D. Cheng, *Chemistry of Materials*, 2005, **17**, 967-973.
28. T. Maitra, S. Sharma, A. Srivastava, Y. K. Cho, M. Madou and A. Sharma, *Carbon*, 2012, **50**, 1753-1761.
29. D. Papkov, A. Goponenko, O. C. Compton, Z. An, A. Moravsky, X. Z. Li, S. T. Nguyen and Y. A. Dzenis, *Advanced Functional Materials*, 2013, **23**, 5763-5770.
30. R. Nain, M. Jassal and A. K. Agrawal, *Composites Science and Technology*, 2013, **86**, 9-17.
31. J. Chen, J. Li, J. Li, G. Xiao and X. Yang, *Journal of Alloys and Compounds*, 2010, **509**, 740-743.

32. H. Wei, Y. Wu, N. Lun and C. Hu, *Materials Science & Engineering, A: Structural Materials: Properties, Microstructure and Processing*, 2005, **A393**, 80-82.
33. B. Cheng and T. Samulski Edward, *Chemical communications (Cambridge, England)*, 2004, 986-987.
34. Z. Song, X. Hou, L. Zhang and S. Wu, *Materials*, 2011, **4**, 621-632.
35. M. Yu, C. Wang, Y. Bai, Y. Wang and B. Zhu, *Journal of Applied Polymer Science*, 2006, **102**, 5500-5506.
36. F. Tuinstra and J. L. Koenig, *The Journal of Chemical Physics*, 1970, **53**, 1126-1130.
37. D. S. Knight and W. B. White, *Journal of Materials Research*, 1989, **4**, 385-393.
38. A. Umair, T. Z. Raza and H. Raza, *arXiv preprint arXiv:1303.6364*, 2013.
39. G. C. Yi, C. Wang and W. I. Park, *Semiconductor Science and Technology*, 2005, **20**, S22-27.
40. O. Lupan, G. Chai and L. Chow, *Microelectronics Journal*, 2007, **38**, 1211-1216.
41. B. Kumar and S.W. Kim, *Nano Energy*, 2012, **1**, 342-355.